High efficiency and wideband gyro-traveling-wave-tube amplifier

Yunyuan Yang[1] and Wu Ding[2]
[1]*Graduate School, China Academy of Engineering and Physics, P.O. Box 2101, Beijing 100088, China*
[2]*Institute of Applied Physics and Computational Mathematics, P.O. Box 8009, Beijing 100088, China*
(Received 9 July 1999; revised manuscript received 26 October 1999)

A model is presented for a wideband gyro-traveling-wave-tube amplifier. The model's output bandwidth is comparable to that of the existing wideband model, but its efficiency is improved a lot. In this model, after choosing a proper initial magnitude, the axial magnetic field has a slightly linear decrease from a given position in the interaction section. The interaction mechanism of the beam wave is analyzed and verified by numerical simulation. When the beam current is 7 A, voltage is 90 KV, the velocity ratio is 1.0, and the axial velocity spread is 2%, numerical results show a constant bandwidth of 20% with an efficiency of 42%; the peak power and gain are, respectively, 260 KW and 47 dB.

PACS number(s): 84.30.Le, 41.75.Fr, 52.75.Ms

I. INTRODUCTION

A gyro-traveling-wave tube (TWT) can produce high frequency output and has high power handling capacity due to its fast-wave interaction. Its bandwidth is wider compared with other gyrotron devices, so the gyro-TWT is the most promising device for the future high resolution radar and high density communication system. But these applications need a wider bandwidth and at the same time a higher gain and efficiency.

There are two major schemes to modify a gyro-TWT for wideband output. The first scheme is the distributed gyro-TWT [1,2]. Both the axial guiding magnetic field and the waveguide cross section should be tapered to maintain synchronism. Using a two-stage structure, a bandwidth of 20% at 35 GHz is achieved, with the peak output power, gain, and efficiency being, respectively, 8 KW, 26 dB, and 16% [1]. In this scheme, it is complex to adjust precisely the magnetic field and the circuit, and if using a single-stage structure, one needs to input the seed signal from the exit. The second one is the dielectric-loaded gyro-TWT. It reduces the circuit dispersion by partly filling the waveguide with a dielectric layer. In Ref. [3] a saturated bandwidth of 14% is obtained at 10 GHz, with the peak output power, gain, and efficiency being 55 KW, 27 dB, and 11%. The dielectric charging effect may appear in this scheme and a waveguide loaded with periodic metal posts [4] was put forward to mitigate this problem. In addition, a two-stream gyro-TWT [5] is put forward for wideband output where two electron beams are inputting simultaneously into the waveguide; its gain is much higher. Spiral waveguides [6] are also used for wideband generation. In this device operation sensitivity to the electron beam spread is reduced a lot.

In this paper we present a model to widen the bandwidth of a gyro-TWT and at the same time increase its efficiency. In this model the initial magnitude of the axial magnetic field B_{0z} is slightly larger than its value B_g at the ''grazing'' point. And from a given position in the interaction section, the axial magnetic field has a slightly linear decrease. It is different from the distributed gyro-TWT that we taper the guiding field only from a given position and the waveguide is uniform; it is also different from the field tapering for efficiency increase [7] because the rule of choice of the initial value of the axial magnetic field is to make the electrons resonate with the radiation field over a wider frequency range. The paper is organized as follows: theoretical analysis and numerical simulation are made in Secs. II and III, respectively; Sec. IV is a brief summary of the paper.

II. MODEL AND ANALYSIS

A. Model

The basic principle of our model is just the same as conventional gyro-TWT's: When a gyrating electron beam travels through a uniform waveguide under the guiding of an axial magnetic field, it stimulates the eigenmode in the waveguide and amplifies the input signal. As we have known, the operating point of a gyro-TWT is often set at the grazing point for high gain and wide instantaneous bandwidth, and the axial guiding field is set slightly below its value B_g at the grazing point. In this paper, in order to broaden the bandwidth further and increase the efficiency, we choose the form of the guiding field as

$$\vec{B}(z)=\begin{cases} B_{z0}\hat{z}, & z<L_0 \\ -\frac{1}{2}B_{z0}\delta r\hat{r}+B_{z0}[1+\delta(z-L_0)]\hat{z}, & z\geqslant L_0. \end{cases} \quad (1)$$

In the entrance section, the guiding field $\vec{B}$ is a constant, $\vec{B}=B_{z0}\hat{z}$; here we demand that B_{z0} is slightly above B_g, $B_g=\omega_c mc\gamma/s\gamma_z e$, where ω_c is the cutoff frequency, γ is the electron's relative mass factor, $\gamma_z=(1-\beta_z^2)^{-1/2}$, $\beta_z=v_z/c$, v_z is the axial velocity of the electrons, c is the light velocity in vacuum, and δ is the amplitude of tapering. From a given position $z=L_0$, the axial magnetic field decreases slightly and a small radical component is generated at the same time. At the end of the interaction section, the axial magnetic field B_z is less than B_g. We define the region $z<L_0$ as the constant region and $z>L_0$ as the taper region.

In the constant region, due to $B_{z0}>B_g$, the dispersion curves of a single waveguide mode and the electron beam mode will have two intersection points A and B at two resonant frequencies ω_{R1} and ω_{R2} (see Fig. 1). The expressions

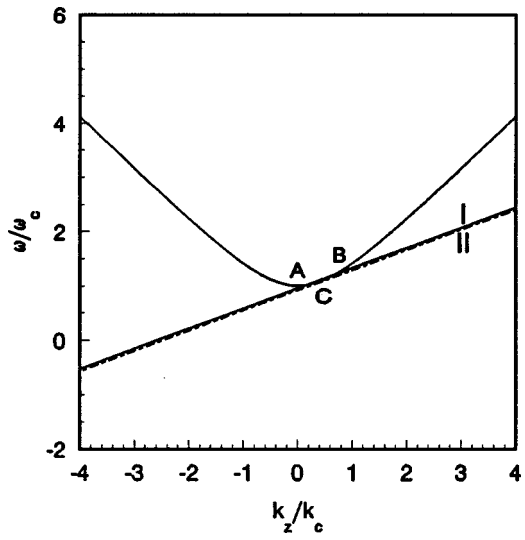

FIG. 1. The dispersion relation between the waveguide and electron beam mode, curve I: $B_z=1.032B_g$; curve II: $B_z=B_g$.

of the two resonant frequencies and their corresponding axial wave numbers are as follows [8]:

$$\omega_{R1,R2}=s\gamma_z^2\Omega\left(1\mp\beta_z\sqrt{1-\frac{1}{\epsilon^2}}\right), \tag{2}$$

$$k_{z1,z2}=s\gamma_z^2\frac{\Omega}{c}\left(\beta_z\mp\sqrt{1-\frac{1}{\epsilon^2}}\right), \tag{3}$$

where s is the electron cyclotron harmonic number, $\Omega=eB_{z0}/mc\gamma$, $\epsilon=s\gamma_z\Omega/\omega_c=B_{z0}/B_g$. Here we require that both k_{z1} and k_{z2} are greater than zero, so both modes with frequencies ω_{R1} and ω_{R2} propagate in the forward direction. From Eq. (3), ϵ should satisfy the condition

$$\epsilon<\gamma_z. \tag{4}$$

Furthermore, we also require that $\epsilon-1$ is small enough that the electron cyclotron line will not intersect with the dispersion curve of the higher waveguide mode nearest to the operating mode. Since the initial magnitude of the axial guiding field we need is just slightly larger than B_g, i.e., $\epsilon\rightarrow1$, the value of ϵ always satisfies the requirements mentioned above for electron beams with moderate voltage and velocity ratio.

On entering the taper region, with the axial guiding field decreasing slightly, the electron cyclotron resonant line slips downward slowly and intersects the waveguide dispersion curve at a series of resonant frequencies. See Fig. 1. When B_z is lowered to B_g, the two dispersion curves are tangential at point C; the relevant frequency ω_{R3} is

$$\omega_{R3}=s\gamma_z^2\Omega_g=\gamma_z\omega_c. \tag{5}$$

With the axial guiding field decreasing further, there are no intersection points anymore. For signals whose frequency is between ω_{R1} and ω_{R2}, there exists a local section where the electron beam can resonate with the signal. According to Eq. (2), we will have

$$\frac{\Delta\omega}{\omega_{R3}}=\frac{\omega_{R2}-\omega_{R1}}{\omega_{R3}}=2\beta_z\sqrt{\epsilon^2-1}. \tag{6}$$

We can see from Eq. (6) that even if ϵ is slightly greater than unit, the electron beam will be able to resonate with the radiation field over a relatively wider frequency range in the waveguide. For example, when $\epsilon=1.032$, the beam voltage $V=90$ KV, the velocity ratio $\alpha=1.0$, $\Delta\omega/\omega_{R3}=19\%$; when $\epsilon=1.024$, $V=135$ KV, $\alpha=1.0$, $\Delta\omega/\omega_{R3}=19\%$. The device will generate wideband output if the signals in the whole unstable frequency range $\Delta\omega$ can be amplified efficiently.

B. Theoretical analysis

In this section we will analyze the amplification mechanism of a signal whose frequency is near ω_{R1}, ω_{R2}, or ω_{R3} in detail. For signals with frequency near ω_{R1} and ω_{R2}, they will be amplified efficiently in the constant region ($z<L_0$) just as conventional cyclotron autoresonance maser amplifier TWT is. Compared with signals with a frequency near ω_{R1}, for signals near ω_{R2}, their axial wave number k_z is relatively large and the axial bunching effect will suppress the azimuthal bunching [9], so the gain is relatively low. Tapering the axial guiding field from a proper position can increase the efficiency and lower the operation sensitivity to the axial velocity spread [7]. In our model, the length of the constant region is close to the saturation length of the signals with frequency near ω_{R2}. For signals with frequency near ω_{R3}, though, the electron beam and the radiation field are markedly off resonance and beam-wave interaction is weak, but due to the existence of both force bunching and inertial bunching, the electron beam may bunch well [10]. When the prebunched electron beam passes through the taper region, there exists a local region where the beam and the radiation field is at or near resonant, so high output power will be generated. In summary, for signals with frequency near ω_{R1} and ω_{R2}, the input signal is amplified preliminary in the constant region and further enhanced in the taper region; for signals with frequency near ω_{R3}, the electron beam is first prebunched in the constant region and releases energy mainly in the taper region.

From the theoretical analysis above, by properly choosing the initial value of the axial magnetic field B_{z0}, the length of the constant region L_0, and the amplitude of tapering δ, high output power will be obtained over a wider frequency range.

III. SIMULATION RESULTS AND DISCUSSION

In this section we will verify by numerical simulation that our model can generate high efficiency and wide bandwidth output. In the simulation process, we assume that the electron beam is an infinite thin ring, its pulse is long enough, and only the first cyclotron harmonic interaction exists, i.e., $s=1$. We select the low loss TE_{01} mode in a circular waveguide as the operating mode, and neglect the space-charge effect. Unless where otherwise stated, the following parameters are used: the electron beam voltage $V=90$ KV, the beam current $I=7$ A, the velocity ratio $\alpha=1.0$, the electron guiding center radius $r_g=0.75r_\omega$, $\mathbf{r}_\omega$ is the radius of the waveguide cross section, the axial velocity spread is 2%, the

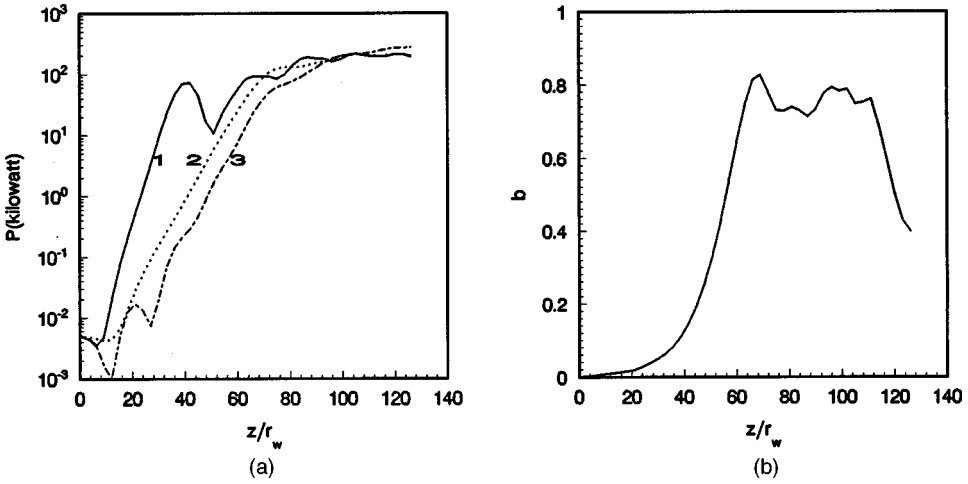

FIG. 2. (a) Radiation power revolution for different frequencies; curves 1, 2, and 3 stand for $\omega/\omega_{R3}=0.94$, 1.0, and 1.12. (b) The bunching parameter b versus the interaction length at $\omega=\omega_{R3}$.

initial magnetic field $B_{z0}=1.032B_g$ ($\epsilon=1.032$), the amplitude of tapering $\delta=0.184\%r_w$(cm), the input power $P_{\rm in}=5$ W, and $L_0=54r_w$. If we specify the center frequency ω_{R3} at 35 GHz, then the waveguide radius $r_w=5.683$ mm and the initial magnetic field $B_{z0}=12.94$ kGs. A frequency sweep is performed to examine the instantaneous bandwidth of the amplifier. The main results are as follows.

In accordance with the theoretical analysis, the amplification characteristics of signals in different frequency ranges are different. From Fig. 2(a), when $\omega\approx\omega_{R1}$, the gain is high and the radiation power has a local maximum before $z=L_0$, which is less than the value at saturation; when $\omega\approx\omega_{R2}$, besides a small decrease at the beginning, the radiation power is amplified gradually with the increasing of the interaction length till saturation; when $\omega=\omega_{R3}$, the radiation power has a great dip at first because the force bunching effect is much stronger than the inertial bunching due to the relatively large off resonance in the entrance section. The radiation power also has a small oscillation before saturation. The bunching parameter b at $\omega=\omega_{R3}$ increases monotoni-

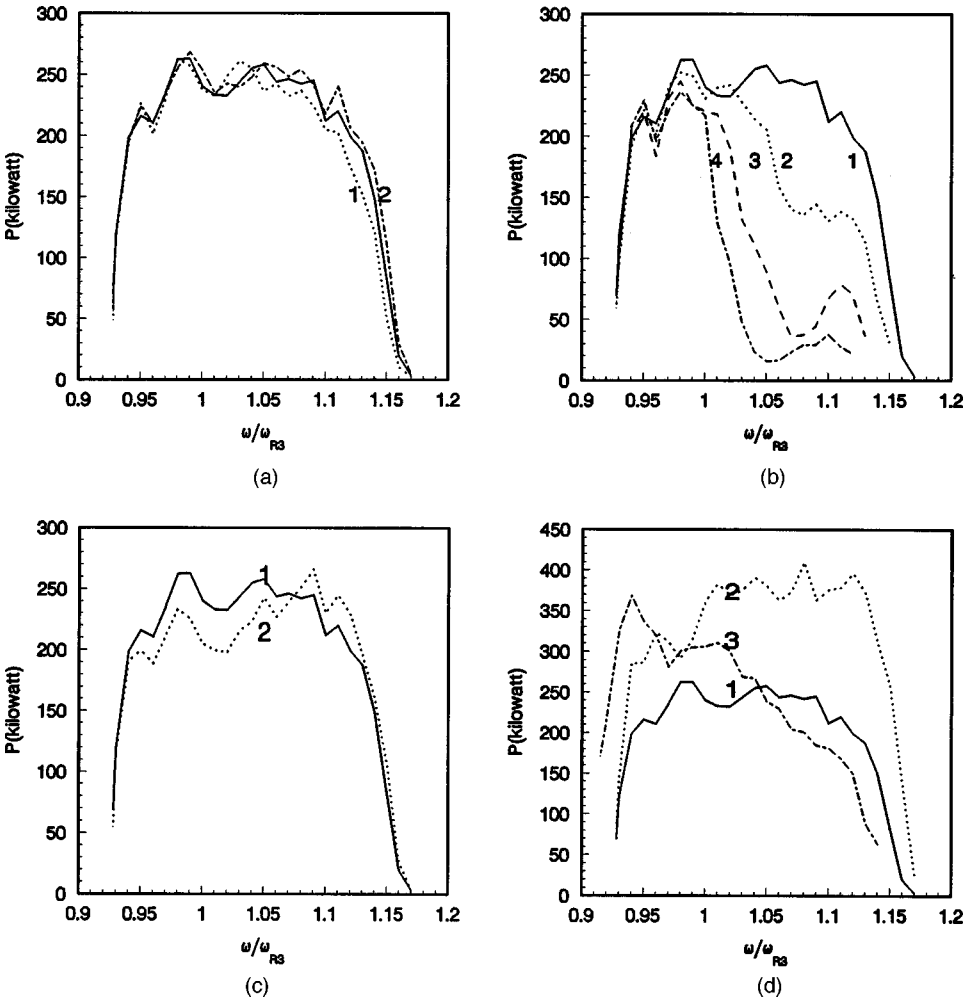

FIG. 3. Output power versus frequency. In (a) curves 1 and 2 stand for $P_{\rm in}=3$ and 7 W; in (b) curves 1, 2, 3, and 4 stand for the axial velocity spreads are 2%, 3%, 4%, and 5%, respectively, relevant $P_{\rm in}$ are 5, 9, 18, and 25 W; in (c) $\delta=0.184\%/r_w$(cm) for curve 1 and $\delta=0.155\%/r_w$(cm) for curve 2; in (d) the beam current $I=7$ Å for curve 1 and $I=10$ Å for curve 2, and the beam voltage $V=135$ KV for curve 3.

cally along the interaction section until it reaches saturation [Fig. 2(b)].

From Fig. 2(a) we can also find that after saturation the synchronous oscillation of the radiation power is relatively small, so the output bandwidth and power are not sensitive to the circuit length. Choosing $L=114r_w$, the calculated constant bandwidth and the efficiency of the amplifier can reach 20% and 42%, respectively, and the peak power and gain are 260 KW and 47 dB. Due to the low loss of the TE_{01} mode, the peak cw wall loading at the end of the last interaction section is less than 100 W/cm^2.

When the input power is varied from 5 W to 3 W or 7 W, from Fig. 3, the output power in the high frequency range increases with the increasing of the input power, while the output power in the low frequency range is almost unchanged. The peak power and bandwidth are 260 KW and 19% when $P_{\rm in}=3$ W and are 268 KW and 20% when $P_{\rm in}=7$ W, respectively; when $\Delta\nu_z/\nu_z=3\%$, the bandwidth is 18% with a peak power 252 KW. Despite the fact that the efficiency at the high frequency range has a relatively large decrease, it is still higher than 20%. When the axial velocity spread increases further [Fig 3(b)], the output power is again affected slightly in the low frequency range, while the output power in the high frequency range has a marked decrease because of large axial wave number k_z, and leads to the relevant decrease of the bandwidth. Though the decrease can be compensated to some extent by increasing the input power, beams with velocity spread less than 4% are wanted in the proposed model. This requirement is not tough considering the development of the magnetron injection gun these days [11]. A high quality beam is a common requirement in most wideband amplifiers [11,12]. Decreasing the peak output power and bandwidth may also be mitigated to some extent by adjusting such parameters as δ, L_0, and r_g.

Fixing all the other parameters, we vary the amplitude of tapering δ from $0.184\%/r_w$ (cm) to $0.155\%/r_w$ (cm); both the peak power and the bandwidth are nearly unchanged [Fig. 3(c)]. When the current is raised to 10 A, we can still achieve wideband and high efficiency output [Fig. 3(d)]. From the results above, we know that the operation of our model is insensitive to such parameters as the amplitude of tapering and beam current. Increasing the beam voltage appropriately, the peak power can be enhanced correspondingly. For voltage $V=135$ KV, $\epsilon=1.024$, other parameters remaining unchanged, the calculated peak power and bandwidth are, respectively, 369 KW and 18%, and the gain and efficiency are 48 dB and 39% [Fig. 3(d)].

Both theoretical analysis and numerical simulation show that our model can generate high efficiency ($\sim$40%) and wideband output ($\sim$20%). The form of the tapering magnetic field it used is simple and not difficult to realize.

In our model, although the initial magnetic field is slightly above its value at the grazing point, it decreases linearly after a relatively short length; thus the stability of the device will not be affected obviously. At present there are many ways to suppress oscillations in a gyro-TWT, and one of the most effective ways is to use a lossy waveguide [13].

IV. CONCLUSION

A model is presented for a wideband gyro-TWT. This model's bandwidth is comparable to that of the existing wideband mode, but its efficiency is improved greatly. The interaction mechanism of the beam wave is analyzed and verified by numerical simulation. When the beam current is 7 A, the voltage is 90 KV, the velocity ratio is 1.0, and the axial velocity spread is 2%, numerical results show a constant bandwidth of 20% with an efficiency 42%; the peak power and gain are, respectively, 260 KW and 47 dB.

[1] G. S. Park *et al.*, Phys. Rev. Lett. **74**, 2399 (1995).

[2] Y. Y. Lau and K. R. Chu, Int. J. Infrared Millim. Waves **2**, 415 (1981).

[3] K. C. Leou, D. B. McDermatt, C. K. Chong, and N. C. Luhmann, IEEE Trans. Electron Devices **43**, 1016 (1996).

[4] K. C. Leou, Tao Pi , D. B. McDermatt, and N. C. Luhmann, IEEE Trans. Plasma Sci. **26**, 488 (1998).

[5] Yunyuan Yang and Wu Ding, Phys. Plasmas **6**, 4328 (1999).

[6] Simon J. Cooke and G. G. Denisov, IEEE Trans. Plasma Sci. **26**, 519 (1998).

[7] K. D. Pendergast, B. G. Danly, R. J. Temkin, and J. S. Wurtele, IEEE Trans. Plasma Sci. **16**, 122 (1998).

[8] *Applications of High Power Microwaves,* edited by Andrei V. Gaponov Grekhov and Victor L. Granatstein (Artech House, Norwood, MA, 1994).

[9] K. R. Chu and A. T. Lin, IEEE Trans. Plasma Sci. **16**, 90 (1988).

[10] P. Sprangle and R. A. Smith, J. Appl. Phys. **51**, 3001 (1980).

[11] K. C. Leou, D. B. McDermott, and N. C. Luhmann, IEEE Trans. Plasma Sci. **20**, 188 (1992).

[12] J. J. Choi, A. K. Ganguly, and C. M. Armstrong, Phys. Plasmas **1**, 2058 (1994).

[13] V. L. Bratmann and G. G. Denisov, Int. J. Electron. **72**, 969 (1992).